# STUDY OF THE STRESS CORROSION CRACKING OF A FERRITIC STAINLESS STEEL AISI-409 WELDED WITH A FILLER METAL FLUX CORED AWS E316LT1-4

**Silva, E.M [1], m_eduardo_silva@yahoo.com.br**
**Costa, S.C [1], sccosta@unifei.edu.br**
**Correa,E.O [1], ecotoni@unifei.edu.br**
**Teixeira, A [5], amauri_t@terra.com.br**
[1,5]Universidade Federal de Itajubá - UNIFEI, Itajubá, Minas Gerais, Brasil.

**Dias, A.O [2], diaswelding@yahoo.com.br**
[2]Universidade Federal de Itajubá - UNIFEI, Itabira, Minas Gerais, Brasil.

**Ribeiro, R.B [3], rosinei1971@gmail.com**
[3]Faculdades Integradas Teresa D'Ávila - FATEA, Lorena, São Paulo, Brasil.

**Rosa, J.R [4], jlrosa@demar.eel.usp.br**
[4]Universidade de São Paulo – USP, DEMAR-ELL, Lorena, São Paulo, Brasil.

***Abstract.*** *The ferritic stainless steel has been extensively applied in chemical and petrochemical industries, automotives parts among others. These ferritic stainless steels present certain advantages compared to austenitic types stainless steel from the family (304, 316…) especially concerning the high resistance to corrosion in certain ways. However, despite of these advantages, in the ferritic stainless steel it is possible to occur some phenomena of embrittlement such as grain growth, formation of sigma phase and carbides precipitation.Thus this study has the aim to evaluate the susceptibility of ferritic stainless steel AISI-409 welded with a flux cored wire AWS E316LT1-4 related with the phenomenon of the stress corrosion cracking (SCC) in aqueous solution containing 43% (weight) $MgCl_2$. The welded specimens were submitted to different levels of heat input (400J/mm, 650J/mm, 708 J / mm and 805J/mm) and the its effect were evaluated. The technique used for tests of SCC was based in a constant load applied during test execution followed by mechanical and microstructural characterization of specimens after failure. The results showed that the region of the weld metal (fusion zone - FZ) presented a higher resistance to the SCC compared wih the heat affected zone (HAZ). Also, the welded specimens with higher heat input (708J/mm and 805J/mm) had better SCC resistance compared with low heat input level (400J/mm), despite their lower cooling rates. It was observed that SCC initially caused cracking in HAZ followed by a propagation to the ferritic region. The microphotograph analysis showed that the ductile-brittle transition is evidenced by low values of elongation. Furthermore, it was observed two distinct regions of fracture, the first being characterized by the presence of dimples, thus underscoring the dúcitl aspect of the fracture, and the second region stands the fragile aspects of the fracture through the cleavage facets due to the phenomenon SCC.*

***Keywords****: Stress Corrosion Cracking, Ferritic Stainless Steel, Welding.*

## 1. INTRODUCTION

The phenomenon of stress corrosion cracking (SCC) occurs when a susceptible material (usually passiveness alloys) is subjected to an applied tensile stress applied or residual stress and exposed to a corrosive environment (Zhou, 1998; Bauernfeind et al, 2004). This phenomenon has been one of the major problems in welded joints of austenitic stainless steels used in environment containing chlorides subjected to high temperatures. This type of catastrophic continuously failure, occurs in important industries such as chemical and petrochemical industry (Alyousif and Nishimura, 2006; Chen et al, 2005; Gertsman and Bruemmer, 2001).

In general, the formation of cracks in stress corrosion occurs at stress level below the yield stress of the material and typically below the design tension and fatigue limit of a structural component (Boven et al, 2007). Because of this phenomenon, resistance to SCC is one of the most important requirements to consider when carrying out welding of austenitic stainless steel. However the SCC, in turn, is strongly influenced by the metallurgical phenomena that occur during welding or even pos-welding when the material is subject to a pos-heat treatment (Sui et al, 1996).

Even the austenitic stainless steel is more susceptible to SCC, the ferritic steel types can be prone to this corrosive phenomenon. In this context the engineering has been prominent in the development of techniques and consumables for welding of ferritic steels with austenitic stainless steels, aiming to combine high resistance to stress corrosion cracking, good thermal conductivity of ferritic and good weldability presented by stainless steel austenitic (Modenesi,2001;Vieira,2006).

According to Lippold and Kotecki (2005) the most important characteristic in choosing a stainless steel for a given application is the resistance to corrosion, greater strength, ductility, weldability, cost and other factors. In this context the austenitic stainless steels exhibit the best combination of mechanical properties and corrosion resistance, but a much higher cost of manufacturing especially in function of the higher nickel price. So, these factors led to the development

and use of ferritic applications where corrosion resistance is higher than that of austenitic grades, such as stress corrosion. Because they have a higher ratio Cr / C, ferritic stainless steels, in general, have better corrosion resistance than the martensitic stainless steels. (Folkhard, 1998).

The ferritic stainless steels have wide application in exhaust systems, piping and equipment operating at high temperature. This exposure to high temperatures has the disadvantage of promote the precipitation of intermetallic phases that compromise its mechanical properties (ductility and toughness) and corrosion resistance. The weldability of these materials has to overcome two basic problems, whether the sensitization (formation of chromium carbides - $Cr_{23}C_6$) that can decrease the corrosion resistance or an irreversible grain growth which in turn can lead to formation of cracks during the solidification process as well as losses in the mechanical properties of heat affected zone. In the first case, the use of alloying elements that reduce the carbon effect in the of chromium carbide formation combined with the thermal cycles allows to contour the situation. In the second case the use of welding conditions that minimize the heat input is essential to minimize the harmful effects of the granulation growth and the excessive deformation.

In this sense, the process control of metal transfer during welding has fundamental importance and among these modes, the condition of pulsed welding reveals itself as an economically viable option for flux cored arc welding. Compared to short circuit transfer mode, the pulsed mode allow an increased deposition rate around 10 to 15% higher (Ghosh et al, 2000). Additionally, the pulsed mode has the advantage of promote grain refinement in the heat affect zone and a better heat control which are fundamental to stainless steel welding.

However, the adjustment of pulse parameters process becomes difficult and the search for welding conditions that result in higher arc stability under these conditions has been the objective of research published in the literature. Based in these aspects this work aims to study the influence of heat input in the susceptibility of ferritic stainless steel AISI-409 with flux cored arc welding AWS E316LT1-4, as the phenomenon of the SCC in aqueous solution containing 43% (weight) $MgCl_2$, seeking for mechanical and microstructural characterization of the joint study.

### 1.1. Microstructural Characterization

It is very well established that a valuable way to predict the microstructure of the weld metal is to use the Schaeffer diagram. Considering the effect of austenite formers and ferrite formers accounted by numerical factors in the chromium equivalent ($Cr_{eq}$) and nickel equivalent ($Ni_{eq}$), the Schaeffer diagram shown in Fig.1 represents the conditions proposed in this research through the welding of a ferritic stainless steel base metal with a filler metal flux cored of austenitic steel. So through testing previously developed by Dias (2009) found that the maximum value achieved for the dilution was 30%, which is used in this work. Therefore note that the weld metal has delta ferrite content around 10%, with the possibility of hardening for the martensite formation.

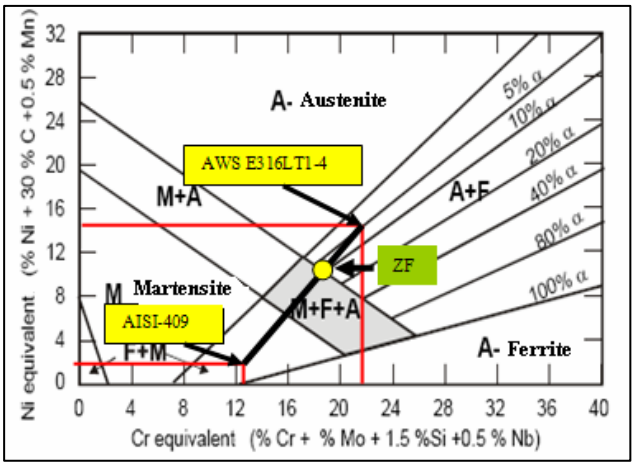


Figure 1. Schaeffler diagram for the welded joint of AISI 409 with filler metal of flux cored wire AWS E316LT1-4.

However, for most applications, the delta ferrite content present at such level has the favorable effect beneficial constituent for the ZF, to reduce or even to avoid completely the tendency to the hot cracking in fusion welding zone during the solidification by its action in promote de dissolution of substances such as sulfur and phosphorus. Such effect, remote the segregation in the grain boundaries of the weld metal and would create starting points for cracks, together with growing tensions inherent in welding. Meanwhile, the negative effect of ferrite in the weld metal is the tendency to be selectively attacked by many corrosive media (Lundqvist, 1977).

The martensite formation in significant content can lead to formation of hydrogen induced cracking, an effect similar to that observed in carbon steels with carbon content exceeding 0.45%. However, few data are yet available in

the literature to confirm this observation on ferritic stainless steels. Moreover, the martensite is still cited as a source of weakness, which can lead to formation of fractures in the base material. However this possibility of formation of martensite becomes larger due to higher cooling rate provided by the lower heat input in the welding tests developed. On the other hand, Lippold and Koteck (2005) report that the combination formed by martensite microstructure and ferrite improves the toughness, when compared whit the total ferritic formation.

## 2. MATERIALS AND EXPERIMENTAL PROCEDURE

In order to achieve the proposed goals in this work, experimental conditions based in a pulsed Flux Cored Arc Welding Process was used. The samples of AISI 409 ferritic stainless steel with dimensions of 130 mm x 65 mm x 3 mm was welded with butt joint, single-V groove and flat position. Austenitic stainless steel flux cored filler metal classified as AWS E316LT1-4 (ESAB OK TUBRIGHT 316L) with a diameter of 1.2 mm were used in all welding conditions. The chemical composition of the steel samples and filler metal are presented in Table 1. Argon-$CO_2$ gas mixture (75% Ar + 25% $CO_2$) was used as shielding gas with a flow rate of 14 l/min. The contact tip to work distance was kept in 22.5 mm. The welding equipment included a digital welding power supply with a welding gun attached to a mechanical tractor to control the moving position. The welding deposition tests were executed using a reverse polarity (DC+) with a fixed voltage level of 23 V. The pulsed parameters used in this research including the peak current (Ip), peak time (tp), base current (Ib) and frequency (f) were fixed from previous optimized welding conditions developed from Dias (2009) and are shown in Table 2. In order to generate different heat inputs, the travel speed (vs) ranged from 22 to 44.3 cm /min.

Considering the welding conditions established, the average current was determined according to equation (1):

$$\mathrm{Im} = \frac{Ip.tp + Ib.tb}{tp + tb} \tag{1}$$

Where tb is the base time and was derived from equation (2):

$$tb = \frac{1}{f} - tp \tag{2}$$

Where f is the pulsing frequency level.

The heat input (H) were derived from the classical welding equation (3):

$$H = \frac{\mathrm{Im}.V}{vs} \tag{3}$$

Where V is the voltage level.

Table 1. Chemical composition (wt %) of the ferritic stainless steel AISI-409 and flux cored arc welding AWSE316LT1-4.

| | **C** | **Si** | **Mn** | **Cr** | **Ni** | **P** | **S** | **N** | **Ti** | **Nb** | **Mo** |
|---|---|---|---|---|---|---|---|---|---|---|---|
| | % | % | % | % | % | % | % | % | % | % | % |
| AISI-409 | 0,03 | 1,00 | 1,00 | 10,50-11,70 | 0,50 | 0,04 | 0,02 | 0,030 | 6xC-0,75 | 0,17 | - |
| AWS 316LT1-4 | 0,03 | 1,00 | 1,58 | 18,5 | 12,4 | - | - | - | - | - | 2,46 |

Table 2. Experimental welding condition.

| **Experiments** | **Ip (A)** | **tp (ms)** | **Ib (A)** | **tb (ms)** | **f (Hz)** | **vs (cm/min)** | **H (J/mm)** |
|---|---|---|---|---|---|---|---|
| 1 | 350 | 2 | 60 | 8 | 100 | 44 | 400 |
| 2 | 350 | 2 | 60 | 8 | 100 | 27 | 650 |
| 3 | 350 | 2 | 60 | 8 | 100 | 25 | 708 |
| 4 | 350 | 2 | 60 | 8 | 100 | 22 | 805 |

After welding, all test specimens were machined for SCC tests according to preparation showed in Fig.2. The samples preparation and test procedures followed the established by ASTM G58-78 and ASTM E8-79 standards. It can be noted that two 8 mm diameter holes spaced 105 mm center to center. The corrosion test was carried out under tension loading device with constant load type, using tensile test specimens without a V-notch like those used in tensile standard test.

The experimental test apparatus consisted of a device with a system for applying constant force on the specimen to be tested. The force is applied through the use of fixed weight and transmitted through the movement of a pulley that drives the main shaft through which the torsion axis moves the lever in a vertical direction. This rotates the support shaft in a counterclockwise direction causing a force of traction acting on the specimen. This force, measured by a load cell is recorded by a digital indicator coupled to the control panel.

As a test procedure, each specimen at time was dipped in a corrosive solution of magnesium chloride ($MgCl_2$) with concentration of 43% inside of a glass cell which is heated by an electric heater at 145 ºC (boiling temperature of the solution), which is recorded by a digital temperature sensor PT-100 in the control panel. The time test until the rupture of the material is recorded by a digital timer. The tension applied axially to the axis of the specimen was 90% of the 0.2% yield strength of ferritic stainless steel AISI409. Each fractured specimen was removed from a sample of 20mm length for the microstructural characterization by optical microscopy and scanning electron microscopy (SEM).

The criterion used to evaluate the susceptibility to stress corrosion in this study was the time of occurrence of total rupture of the specimens and the applied load.

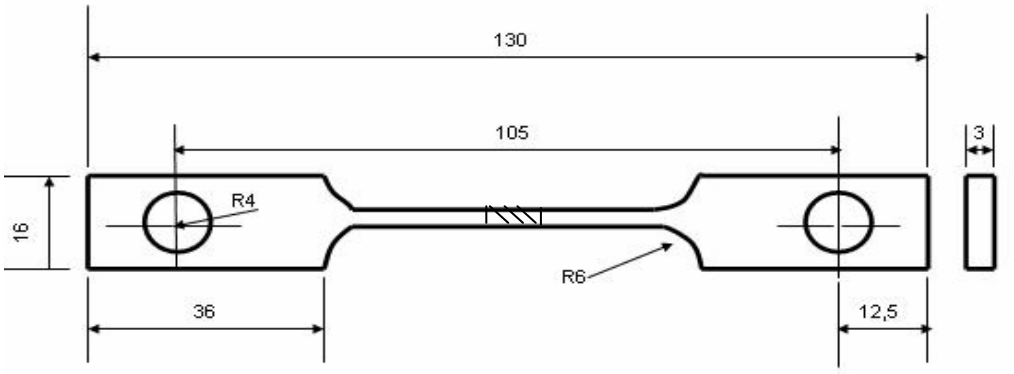


Figure 2. Design of the smooth tensile specimen used in SCC tests. Units: mm.

## 3. RESULTS AND DISCUSSION

### 3.1. Microstructure

The Fig.3 shows the microstructure of heat affected zone (HAZ) to heat input of 805J/mm, being this formed by polygonal ferrite grains. There is also the precipitation of carbides type $M_{23}C_6$ in grain boundaries in the HAZ region.

It is worthy while that the precipitation of carbides results in compositional heterogeneities in the region of grain boundaries making these areas anodic in relation to the remain of the grain and in such a way it speeds up still more the development of corrosion cracks, because it is possible to perceive that in these regions are points of stress concentration.

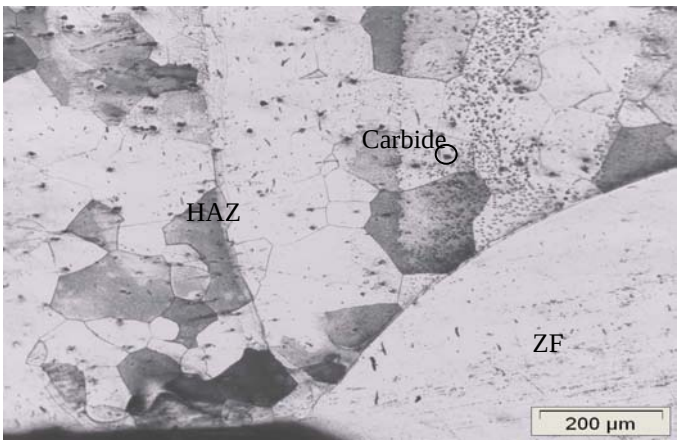


Figure 3. Microstructure of heat affected zone and fusion zone. H= 805J/mm.
Etching: Reagent Marble, attack time 40s, 100X.

Fig.4 shows the microstructure of weld metal, which exhibited varying amounts of delta ferrite in each sample analyzed. It can be observed that the number of delta ferrite (ranged from 6.4 to 7.0) were different for each heat input used as Table 3. In general there is a continuous network of vermicular delta ferrite in both the welds with low and high heat input. So, the amount of delta ferrite must be controlled in applications where the weld needs a good corrosion resistance, high toughness in the weld at low temperatures and when the part can not have the presence of any residual magnetism.

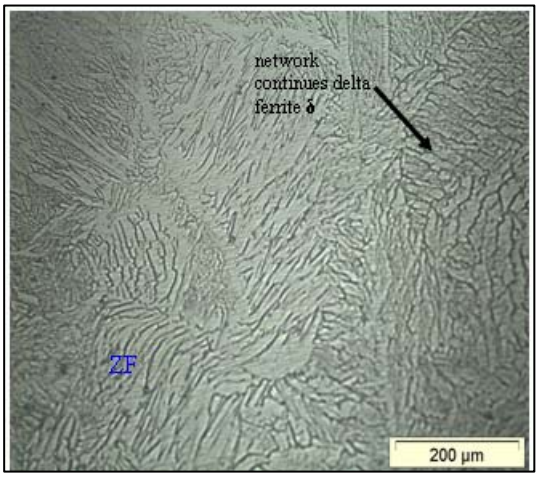


Figure 4. Microstructure of the specimen welded with H = 400J/mm.
Etching: Electrolytic time 2min and 30s, 100x

Table 3. Measurement of ferrite content in the HAZ using the method of ferrography.

| Heat input(J/mm) | Delta ferrite (%) |
|---|---|
| 400 | 6,4 +/- 0,250 |
| 650 | 6,6 +/- 0,243 |
| 708 | 6,5 +/- 0,317 |
| 805 | 7,0 +/- 0,295 |

Correa et al (2010), in their studies found that the interference of the presence of delta ferrite in austenitic welds with susceptibility to stress corrosion cracking was more related to their shape and distribution in the austenitic matrix than with its content. But for the tests studied it was observed that the welds made with low heat input (H = 400J/mm) had a lower delta ferrite content compared with welds with the highest heat input (H = 805J/mm). This probably is due to higher cooling rate that these joints were subjected. But controlling the amount of delta ferrite in stainless steel welds is very critical, because if there is an excessive amount of delta ferrite (more than 10% by weight) there is a reduction of ductility, mechanical strength and corrosion resistance if the amount of delta ferrite is very low (less than 5% by weight) there is an increased incidence of hot cracks during solidification of the weld metal.

### 3.2. Microhardeness

The microhardness in the welded joint can represent a variety of behaviors to which the structure of the material was submitted, and can be influenced by several aspects, including the thermal cycle imposed during the welding, the chemical composition of filler metals and the equivalence between the mechanical properties of weld metal and the base metal. Generally, the HAZ, especially in the area adjacent to the melted line, has a tendency to be hardened due to the welding process (Tsay et al, 2001).

The Fig.5 shows the behavior of the hardness of the welds under the effect of different heat inputs. The micro hardness was measured horizontally through the cross section of the samples at various points observing the following procedure: the points 1, 3, 8 and 9 = Mb; 4, 5, 6, and 7 = HAZ.

Analyzing the Fig.5, it is possible to observed that the weld made with lower heat input (H = 400J/mm), showed a trend to higher hardness, which was expected due to more rapid cooling rate experienced by this welds, and also because the presence of some chemical elements present in the weld metal.

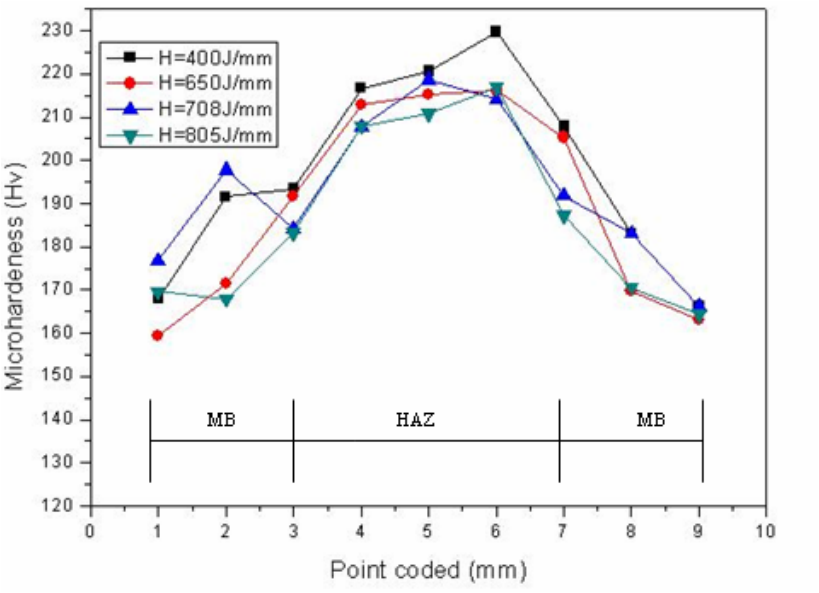


Figure 5. Vickers hardness behavior to the points coded.

Table 3. Variation of the average micro hardness tests for welding

| Points coded | d1 ($HV_{0,2}$) | s | d2 ($HV_{0,2}$) | s | d3 ($HV_{0,2}$) | s | d4 ($HV_{0,2}$) | s |
|---|---|---|---|---|---|---|---|---|
| 1 | 167,9 | 2,26 | 159,3 | 12,82 | 176,8 | 11,88 | 169,7 | 11,53 |
| 2 | 191,6 | 1,20 | 171,5 | 8,23 | 197,8 | 26,73 | 167,9 | 10,36 |
| 3 | 193,4 | 19,52 | 191,8 | 0,85 | 184,2 | 4,10 | 183,2 | 18,73 |
| 4 | 216,7 | 1,27 | 212,8 | 8,34 | 207,7 | 12,52 | 207,9 | 12,66 |
| 5 | 220,6 | 5,56 | 215,3 | 22,84 | 218,6 | 21,64 | 210,8 | 18,24 |
| 6 | 229,7 | 4,50 | 216,1 | 25,53 | 214,1 | 24,11 | 216,9 | 21,85 |
| 7 | 207,8 | 3,50 | 205,3 | 16,17 | 191,8 | 17,54 | 187,3 | 15,63 |
| 8 | 183,2 | 7,92 | 169,7 | 19,16 | 183,2 | 7,92 | 170,6 | 14,07 |
| 9 | 166,1 | 1,48 | 163,2 | 9,10 | 166,1 | 2,90 | 164,4 | 11,24 |
| **Heat input (J/mm)** | **400** | | **650** | | **780** | | **805** | |

The Table 3 shows that the maximum micro hardness was 230 HV including all welding conditions, which was considered as an acceptable level according to the criteria adopted by the standard NACE MR015 (2001), which establishes the maximum hardness of 250 HV for materials metal used in petroleum equipment in order to avoid stress corrosion cracking in media containing $H_2S$.

### 3.3. Stress Corrosion Cracking

The Table 4 shows the results obtained after metallographic analysis of specimens tested for SCC in solution of magnesium chloride 43% by weight.

It can be noted that there is a very similar behavior of the specimens for resistance SCC for chlorides and note that when it arrives in welding heat input as an increase in the time of rupture of the analysed samples. It can be noted that the heat input has a significant effect on the susceptibility of fracture failure. The use of lower heat input has an important impact in increase the risk of fracture characterized by a smaller time to failure. Maybe this fact can be explained by the faster cooling rate in this welding condition which results in microstructural formation more susceptible to fracture. On the other hand, the increase in the heat input reveals a tendency in reducing the risk of fracture with a clear tendency of stabilization for the conditions of higher heat input (708 e 805 J/mm). Meanwhile more tests needs to be realized to reinforce this hypothesis.

However, it can be noted that all samples analysed were broken almost in its totality in the HAZ, independent of the energy applied, making this region more susceptible to corrosion cracking. Probably this occurred because this region is subject to a fast thermal cycle, which produces metallurgical modifications in its structure, such as precipitation of carbides and phases formations, beyond irreversible growth of the grain sizes.

Table 4. SCC tests results on specimens welding.

| Experiments | Heat input J/mm) | Rupture time (min) | Temperature (ºC) | Region | Frature |
|---|---|---|---|---|---|
| 1 | 400 | 3649 | 145 | HAZ | Brittle |
| 2 | 650 | 5333 | 145 | HAZ/ZF | Ductile-brittle |
| 3 | 708 | 7887 | 145 | HAZ/ZF | Ductile-brittle |
| 4 | 805 | 7280 | 145 | HAZ/ZF | Ductile-brittle |

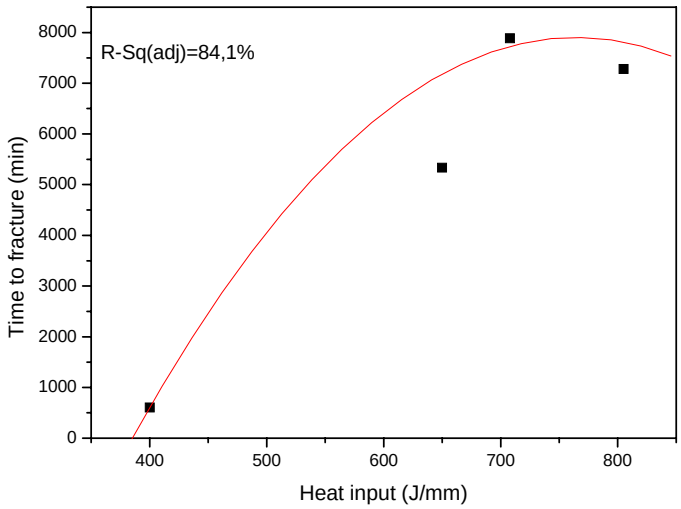


Figure 6. Influence of the heat input on the time to fracture.

### 3.4. Fractografy

Through the microscopic analysis in the fractured region Fig. 7 (a and b), it was identified two distinct regions, one from the corrosion process and the other coming from the fracture mechanism due to increased tension originated by the reduction in the area of the specimen. Note that the samples showed a region with aspect ductile-fragile.

Moreover, there are presences of dimples, emphasizing the aspect of fracture ductile. The micrographs obtained by (SEM) highlight the fragile aspect of the fracture through the facets cleavage, indicates that the phenomenon of SCC contributed to the fracture of the material.

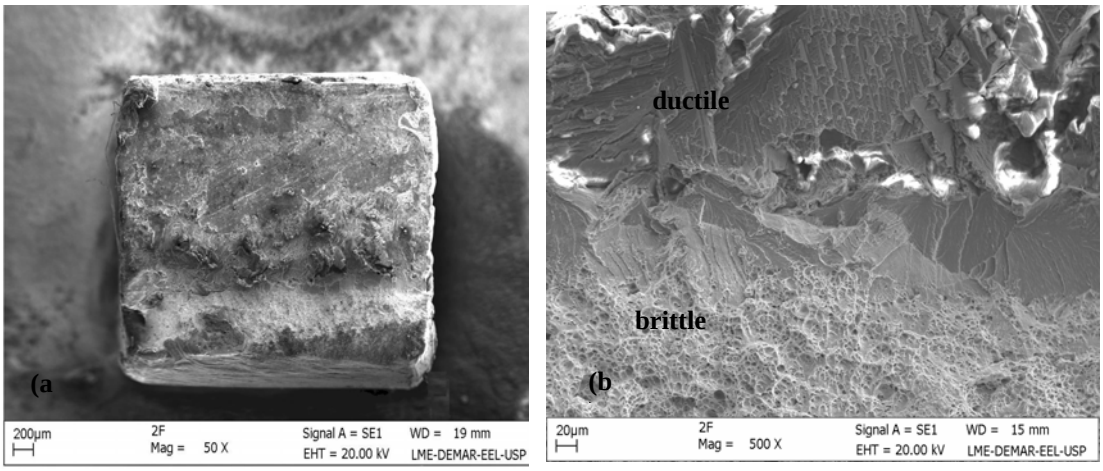


Figure 7. Characterization of the ductile-brittle fracture transition H= 650J/mm.

The crack morphology after metallographic examinations allows observing that the crack predominantly propagated through the interior of grains characterized by a transgranular fracture type with multiple branches as shown in Fig. 8 (a and b). The crack propagation always occurs in the direction perpendicular to the applied force and the path of broken intergranular fracture SCC it was not observed. Probably this was occurred because the ferritic region, which exhibits considerable plasticity, making it difficult allowing crack propagation by the presence of a region of good resistance, resulting in a longer time to fracture the material (Pinto, 2006).

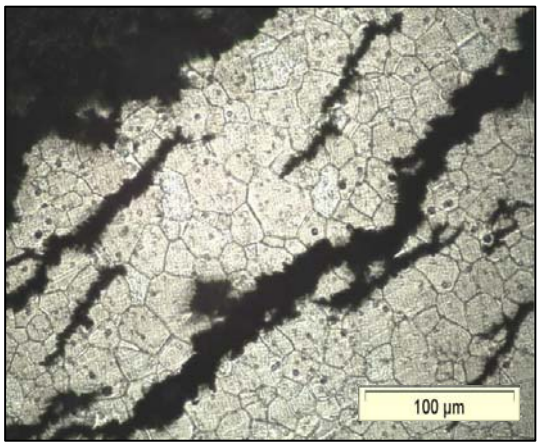


Figure 8.Transgranular cracking of SCC in the region of HAZ, H = 400J/mm.Etching electrolytic, 200x increase.

A more detailed analysis of the cracked region was made with the aid of SEM , Figs.9 (a and b). It can be noted the presence of many microcracks, localyzed in the grain boundaries in HAZ region. These results indicate that the deposited weld metal originated from a tubular austenitic wire resulted in a decreasing in a resistance to cracking caused by SCC.

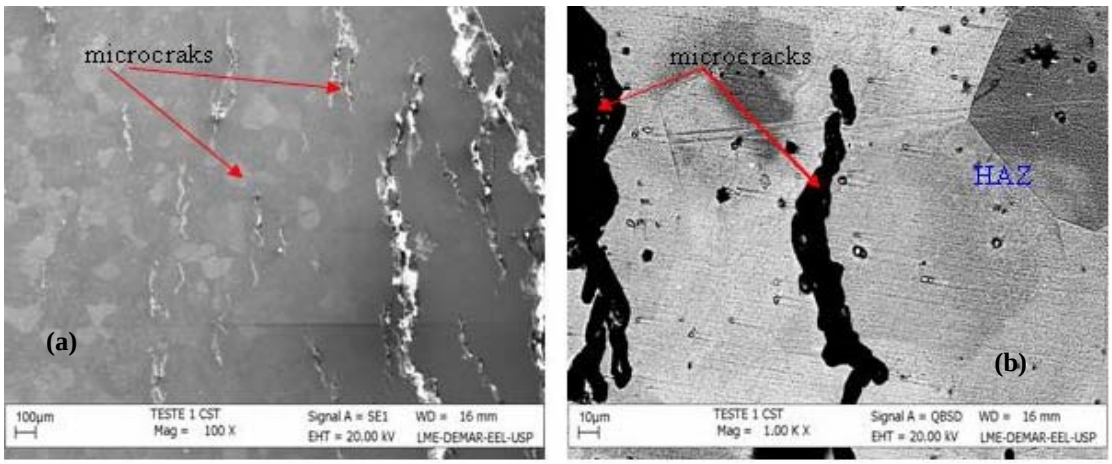


Figure 9. Microcracks in the region of HAZ, H = 400J/mm.

## 4. CONCLUSIONS

1) Welds made with less heat input showed a tendency to have a higher hardness in the HAZ, due mainly to precipitation of carbides in the ferrite grain boundaries, this probably contributed to the decrease in resistance to SCC, as these regions become anodic relative to the rest of the material, favoring the mechanism of anodic dissolution resulting the cracking SCC.
2) Welds made with the highest heat input showed greater resistance to stress corrosion cracking, but the small difference between the values of input used, does not allow this result to be considered indiscriminately.
3) The morphology of the crack, the metallographic analysis revealed that the cracks were predominantly transgranular, with many branches, and these began in the weld metal (austenitic) and spread to the base metal (ferritic).

## 5. ACKNOWLEDGEMENTS

The authors are grateful to Arcelor Mittal Inox by providing the material and the CNPq and FAPEMIG for the financial support to this project.

## 6. REFERENCES

Alyousif, O.M. and Nishimura, R., 2006, "The Effect of Test Temperature on SCC Behavior of Austenitic Stainless Steel in Boiling Saturated Magnesium Chloride Solution". Corrosion Science, Vol.48, pp.4283-4293.

ASTM G58-78**,** "Standard Practice for the Preparation of Stress Corrosion Test Specimens for Weldments".Annual Book of ASTM Standards, American Society of Testing and Materials.

ASTM E8-79**,** "Standard Metholds of Tension Testing of Metallic Materials".Annual Book of ASTM Standards, American Society of Testing and Materials.

Bauernfeind, D., Romotowski, J., Haberl, J., Mori, G., Bernauer, J., Saller, G., 2004, "Stress Corrosion Cracking of Highly Alloyed Austenitic Stainless Steel in Chloride Media". University of Leoben, Austria, pp.1-8.

Boven, G.V., Chen, W., Rogge, R., 2007, "The Role of Residual Stress in Neutral pH Stress Corrosion Cracking of Pipeline Steels-Part I: Pitting and Cracking Ocurrence". Acta Materialia, Vol.55, pp.29-42.

Chen, Y.Y., Liou, Y.M., Shih, H.C., 2005, "Stress Corrosion Cracking of Type 321Stainless Steels in Simulated Petrochemical Process Environments Containing Hydrogen Sulfide and Chloride". Materials Science and Engineering A,Vol. 407, pp.114-126.

Correa,E.O., Barbosa,R.P., Buschinelli,A.J.A., Silva,E.M.,2010, "Influence of Clad Metal Chemistry on Stress Corrosion Cracking Behaviour of Stainless Steels Claddings in Chloride Solution", Scientific Research,Vol.2,pp.391-396.

Dias, A.O, 2009, "Análise dos Parâmetros de Soldagem do Aço Inoxidável AISI 304 através do Eletrodo Tubular AWS E316LT1-4 no Modo de Transferência Pulsado". Dissertação de Mestrado, Universidade Federal de Itajubá – UNIFEI, 115 p.

Folkhard, E., "Welding Metallurgy of Stainless Steels", 1998, New York, Spring-Verlag Wien

Gertsman, V.Y. and Bruemmer, S.M.,2001, "Study of Grain Boundary Character Along Intergranular Stress Corrosion Crack Paths in Austenitic Alloys".Acta Materialia,Vol.49,pp.1589-1598.

Ghosh,P.K., Gupta,S.R., Randhawa,H.S., 2000,"Characteristics of a Pulsed-Current,Vertical-Up Gas Metal Arc Weld in Steel", Metallurgical and Materials Transactions,Vol.31A, September,pp2247-2256.

Lippold, J.C. and KoteckiI, D.J., 2005, "Welding Metallurgy and Weldability of Stainless Steels", John Willey & Sons, 356p.

Lundqvist,B., 1977, "Soldagem dos Aços Inoxidáveis nas Indústrias de Celulose e Papel",Soldas e eletrodos,Jun,pp.8-18.

Modenesi, P.J., 2001, "Soldabilidade dos Aços Inoxidáveis", São Paulo, 2001, SENAI-SP, Coleção Tecnologia da Soldagem, Vol.1, 100p.

NACE MR0175, 2001, "Petroleum and Natural Gas Industries Materials for Use in $H_2S$-Containing Environments in Oil and Gas Production".The Corrosion Society,USA, First Edition,144p.

Pinto, D.F. 2006, "Comportamento em Corrosão sob Tensão de um Aço Inoxidável Ferrítico AISI444 Soldado com Aço Inoxidável Austenítico AISI316LSi em Meios Contendo Cloretos". Dissertação de Mestrado, Universidade Federal de Ouro Preto,106p.

Sui,G., Charles,E.A., Congleton,J.,1996, "The Effect of Delta-Ferrite Content on the Stress Corrosion Cracking oj Austenitic Stainless Steels in a Sulphate Solution".Corrosion Science, Vol.38,n˚5,pp.687-703.

Tsay,L.W., Chen,Y.C., Chan,S.L.I., 2001, "Sulfide Stress Corrosion Cracking and Fatigue Crack Growth of Welded TMCP API 5LX65 Pipe-Line Steel",International Journal of Fatigue,Vol.23,pp.103-113.

Vieira, D.H.P., Carvalho, D.F., Bálsamo, P.S.S., Godefroid, L.B., Cândido, L.C., 2006, "Comportamento em Corrosão de Juntas Soldadas de Aços Inoxidáveis em Meios contendo Íons Cloretos", Tecnologia em Metalurgia e Materiais, Vol.3, n˚2, out-dez, p.6-10.

Zhou**,** W., 1998, "Stress Corrosion Cracking Causes and Solutions". Singapore Welding Society, Newsletter, September, pp.1-6.

## 7. RESPONSIBILITY NOTICE

The authors are the only responsible for the printed material included in this paper.